





## Article

# Diurnal Evapotranspiration and Its Controlling Factors of Alpine Ecosystems during the Growing Season in Northeast Qinghai-Tibet Plateau

Qiwen Liao <sup>1,2</sup>, Xiaoyan Li <sup>1,2,3,4,\*</sup>, Fangzhong Shi <sup>1,2</sup>, Yuanhong Deng <sup>1,2</sup>, Pei Wang <sup>1,2</sup>, Tingyun Wu <sup>1,2</sup>, Junqi Wei <sup>1,2</sup> and Fenglin Zuo <sup>1,2</sup>

- <sup>1</sup> State Key Laboratory of Earth Surface Processes and Resource Ecology, Beijing Normal University, Beijing 100875, China; liaoqw20@outlook.com (Q.L.); fzshi@mail.bnu.edu.cn (F.S.); dengyuanhong525@gmail.com (Y.D.); peiwang@bnu.edu.cn (P.W.); twinklewu@outlook.com (T.W.); 201731190017@mail.bnu.edu.cn (J.W.); flzuo@bnu.edu.cn (F.Z.)
- <sup>2</sup> School of Natural Resources, Faculty of Geographical Science, Beijing Normal University, Beijing 100875, China
- <sup>3</sup> Key Laboratory of Tibetan Plateau Land Surface Processes and Ecological Conservation, Ministry of Education, Qinghai Normal University, Xining 810016, China
- <sup>4</sup> Academy of Plateau Science and Sustainability, Qinghai Normal University, Xining 810016, China
- \* Correspondence: xyli@bnu.edu.cn



**Citation:** Liao, Q.; Li, X.; Shi, F.; Deng, Y.; Wang, P.; Wu, T.; Wei, J.; Zuo, F. Diurnal Evapotranspiration and Its Controlling Factors of Alpine Ecosystems during the Growing Season in Northeast Qinghai-Tibet Plateau. *Water* **2022**, *14*, 700. <https://doi.org/10.3390/w14050700>

Academic Editors: Yaning Chen, Bin He, Zhi Li, Gonghuan Fang and Weili Duan

Received: 22 December 2021

Accepted: 21 February 2022

Published: 23 February 2022

**Publisher's Note:** MDPI stays neutral with regard to jurisdictional claims in published maps and institutional affiliations.



**Copyright:** © 2022 by the authors. Licensee MDPI, Basel, Switzerland. This article is an open access article distributed under the terms and conditions of the Creative Commons Attribution (CC BY) license (<https://creativecommons.org/licenses/by/4.0/>).

**Abstract:** It is generally believed that evapotranspiration at night is too miniscule to be considered. Thus, few studies focus on the nocturnal evapotranspiration ( $ET_N$ ) in alpine region. In this study, based on the half-hour eddy and meteorological data of the growing season (from May to September) in 2019, we quantified the  $ET_N$  of alpine desert (AD), alpine meadow (AM), alpine meadow steppe (AMS), and alpine steppe (AS) in the Qinghai Lake Basin and clarified the different response of evapotranspiration to climate variables in daytime and nighttime with the variation of elevation. The results show that: (1)  $ET_N$  accounts for 9.88~15.08% of total daily evapotranspiration and is relatively higher in AMS (15.08%) and AD (12.13%); (2) in the daytime, net radiation ( $R_n$ ), temperature difference ( $TD$ ), vapor pressure difference ( $VPD$ ), and soil moisture have remarkable influence on evapotranspiration, and  $R_n$  and  $VPD$  are more important at high altitudes, while  $TD$  is the main factor at low altitudes; (3) in the nighttime,  $VPD$  and wind speed ( $WS$ ) control  $ET_N$  at high altitudes, and  $TD$  and  $WS$  drive  $ET_N$  at low altitudes. Our results are of great significance in understanding  $ET_N$  in the alpine regions and provide reference for further improving in the evapotranspiration estimation model.

**Keywords:** evapotranspiration; nighttime; Qinghai Lake Basin; eddy covariance observation

## 1. Introduction

Evapotranspiration ( $ET$ ), as one of the key and complex links in the process of hydrological cycle and energy cycle, is an active factor affecting regional hydrology, climate, and soil [1]. Defined as the total water vapor flux transported to the atmosphere by vegetation and ground,  $ET$  mainly includes the soil evaporation and vegetation transpiration [2]. Soil evaporation is the process of soil water rising from the soil surface into the atmosphere, which is mainly affected by solar radiation, temperature, relative humidity ( $RH$ ), wind speed ( $WS$ ), and soil texture. Transpiration of vegetation is the main cause of water loss in vegetation, which is related to photosynthesis and respiration of vegetation [3,4]. Due to the lack of effective observations, traditional studies widely concluded that stomata of most plants were completely closed, and transpiration was impossible after sunset because of the absence of solar radiation for driving transpiration at night. Thus, water loss from the ground into the atmosphere at night was often overlooked [5–7]. However, studies have shown that nocturnal transpiration is possible and has been measured in both woody and

herbaceous plants [8–11]. Actually, the nocturnal  $ET$  ( $ET_N$ ) includes soil evaporation and plant transpiration as that in the daytime. Increasing evidences indicated that incomplete stomatal closure exists, and the subsequent transpiration overnight is very common, which would result in 10~15% of daytime plant water loss at night [12]. Moreover, water loss at night can even reach 25~30% in deserts and savannas [13,14]. For soil evaporation, driven by the reduction of land surface temperature (cold end) and increase in the surface soil water tension, which means a lower soil water potential, unsaturated soil water migrates from the warm deep (soil inside) to the cold end (land surface) [15]. Thus, evaporation could occur at the night, while the soil temperature is low. Therefore,  $ET_N$  plays an important role in the quantification of  $ET$ , whose neglect would lead to the underestimation of ecosystem evaporation [16,17].

The intensity of regional  $ET$  is affected by plant growth conditions (leaf area index), sources (soil moisture), and energy driving force (solar radiation) [3,4,18]. Since there is no solar radiation at night, the main control factors of  $ET$  are different between day and night. Most studies have shown that the influencing factors of daily  $ET$  ( $ET_D$ ) mainly include air temperature ( $T_a$ ), vapor pressure difference ( $VPD$ ), and  $WS$ , while the driving factors of  $ET_N$  are mainly controlled by  $VPD$  and ventilation conditions [19,20]. At present, there are few studies focusing on  $ET_N$  and its influencing factors, especially alpine regions, which have intense solar radiation during the daytime and large temperature difference between day and night. The quantification in  $ET_N$  and exploration of the potential mechanisms are urgent gaps in the study of the hydrological cycle and water budget of alpine ecosystem.

The Qinghai-Tibet Plateau has a unique alpine environment and various ecosystems, including alpine shrubs, alpine steppe, alpine meadow, and alpine desert, which makes it sensitive and vulnerable to climate change [21,22]. However, current studies related to  $ET$  mostly focus on forests [23,24], wetland [25], and farmland [26–28]. There are relatively few studies on  $ET$  in cold alpine ecosystems. In recent years, the climate of the Qinghai-Tibet Plateau has undergone great changes, altering the hydrological cycle and the energy cycle [29]. Although wind stilling could result in decrease in  $ET$ , the warming of  $T_a$  and land surface temperature and increase in ground-air temperature gradient [29], soil moisture, and vegetation density led to more evaporation on the Qinghai-Tibet Plateau [29–31]. For example, Yin et al. [32] reported that the actual  $ET$  over the Qinghai-Tibet Plateau increased at rate of  $0.08 \text{ mm}\cdot\text{a}^{-1}$  in the past 30 years by model simulation. However, most existing studies in  $ET$  are based on remote sensing inversion and model simulation, which have great uncertainty in regional upscaling [33,34], and remote sensing inversion can only be carried out on a coarse time scale and is restricted to quantify the diurnal variation of  $ET$  [35]. Therefore, the acquisition and analysis of multi-site and high-frequency observed data are very important in the study of regional  $ET$ . There are many methods to calculate  $ET$  based on fully physical models, semi-physical models, and black-box models [36,37]. The calculation methods are relatively reliable by fully physical models that account for mass and energy conservation principles [38]. Eddy covariance ( $EC$ ) method is the most accurate observation method internationally recognized, with relatively large spatial representativeness, which has perfect theoretical verification and can continuously observe the actual  $ET$  at high frequency for a long time [39,40] and has been an ideal method to explore the characteristics and potential mechanisms of actual  $ET$  at different time scales [41–43]. It calculates  $ET$  through the observed latent heat flux by the  $EC$ , which is based on the mass and energy conservation principles [43]. However, in the alpine region, due to its harsh climate and environmental conditions, it is more difficult to install and maintain instruments, and observation stations are very scarce at the regional scale. Therefore, it is exigent to explore the changes and influencing factors of  $ET$  at different time scales in alpine regions through high-frequency observation of  $ET$  at multiple stations on the watershed scale.

Qinghai Lake Basin, with typical alpine ecosystems, is a representative alpine area of Qinghai-Tibet Plateau; thus, the study of  $ET$  of alpine ecosystems in the Qinghai Lake Basin is key to understanding the  $ET$  process of alpine ecosystems in the Qinghai-Tibet

Plateau and is of great significance to the assessment of water resources in the Qinghai-Tibet Plateau. With typical fragile ecosystems, Qinghai Lake Basin is situated in the northeastern Qinghai-Tibet Plateau and is sensitive to climate change [44]. In recent years, the water level of Qinghai Lake continues to rise [45], and with the emergence of problems, such as soil erosion and grassland degradation, the water balance in the basin has always been a research focus. As an important component of water balance, *ET* has attracted more and more attention. Based on the half-hourly eddy covariance and micrometeorological data of alpine desert (AD), alpine meadow (AM), alpine meadow steppe (AMS), and alpine steppe (AS) of the growing season (from May to September) in 2019 over Qinghai Lake Basin, we aim to (1) quantify and compare the *ET* of the four typical alpine ecosystems during daytime and nighttime and (2) identify the influencing factors for *ET* during daytime and nighttime with the variation of elevation.

## 2. Materials and Methods

### 2.1. Site Description

Qinghai Lake Basin is located in the northeast of the Qinghai-Tibet Plateau (Figure 1) and lies in the high altitude, cold, and semiarid climate zone characterized by windy conditions, strong solar radiation, a large temperature difference between day and night, and rainfall that mainly occurs in summer. The mean annual  $T_a$  ranged from  $-1.34\text{ }^{\circ}\text{C}$  to  $-0.1\text{ }^{\circ}\text{C}$  and increased by  $0.03\text{ }^{\circ}\text{C}\cdot\text{a}^{-1}$  during 2001~2015 [44,46]. The mean annual precipitation and evaporation were about 400 and 1000 mm, respectively, and both of them happen mainly in the growing season from May to September (more than 85% and 60%, respectively) [44,47]. Four observation sites were selected in the Qinghai Lake Basin and detailed through information in Table 1, which were characterized by cold alpine ecosystems (AD, AM, AMS, and AS), respectively. They account for more than 75% of the total land area of the whole watershed [48,49].

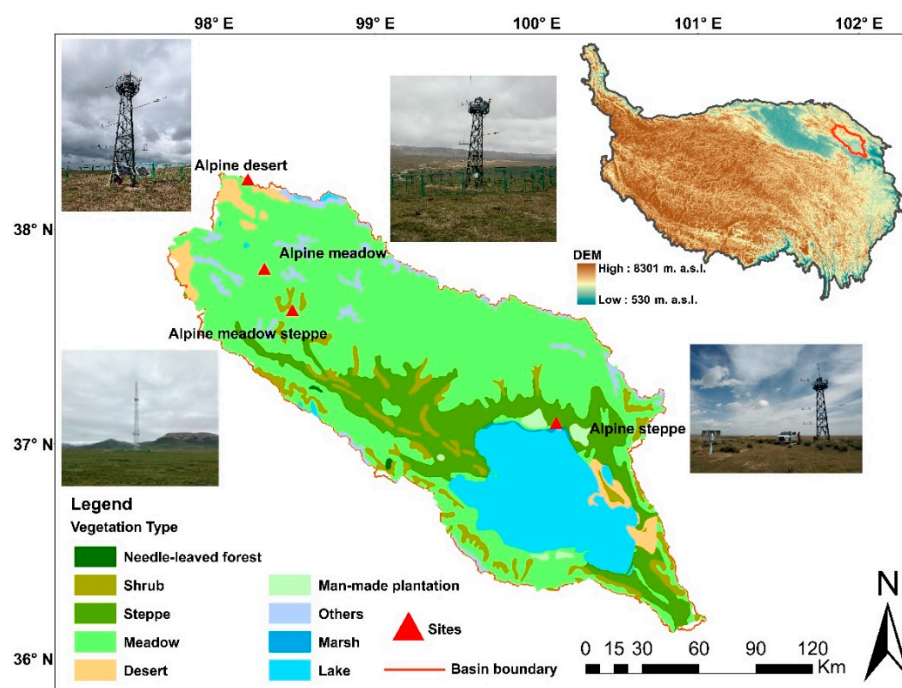


Figure 1. Location of Qinghai Lake Basin and observation sites.

**Table 1.** Information regarding location, altitude, soil, and vegetation in four ecosystems. The soil was classified according to the Chinese soil taxonomy.

Ecosystem	Geographical Coordination	Altitude /m. a.s.l.	Soil Type	Plant Species
Alpine Desert	38°17′55.77″ N, 98°16′10.97″ E	4211	Haplic Cryo-sod Soil	<i>Rhodiola tangutica</i>
Alpine Meadow	37°53′12.75″ N, 98°24′28.21″ E	3974	Mat Cryo-sod Soil	<i>Kobresia humilis</i>
Alpine Meadow Steppe	37°42′10.30″ N, 98°35′38.10″ E	3718	Mat Cryo-sod Soil	<i>Kobresia humilis</i> ; <i>Stipa purpurea</i>
Alpine Steppe	37°14′49.00″ N, 100°14′8.99″ E	3205	Cal-Ustic Isohumisols	<i>Achnatherum splendens</i>

## 2.2. Instrumentations

We built observation towers at four sites separately, with *EC* systems comprised of three-dimensional sonic anemometer (Model CSAT3 (Campbell Scientific Inc., Logan, UT, USA), Wind Master Pro (Gill Instrument Limited Hampshire, Lymington, UK)) and open-path infrared gas analyzer (Model EC150 (Campbell Scientific Inc., Logan, UT, USA), Li-7500 (Model Li-Cor, Lincoln, NE, USA)), installed 4.5 m above the ground. The data were collected at 10 Hz by CR1000X data loggers (Model Campbell Scientific Inc., Logan, UT, USA). The observation data of *EC* mainly include latent heat flux (*LE*), sensible heat flux (*H*) and net ecosystem exchange (*NEE*).

Observations of near-surface meteorological elements are measured by a set of automatic weather stations, including *Ta* and *RH* (Model HMP155, Vaisala Inc., Helsinki, Finland), *WS* (Model Windsonic, Gill Instrument Limited, Hampshire, UK), precipitation (*Pre*, Model T-200b, Geonor Inc., Oslo, Norway), land surface temperature and soil temperature (*LST/Ts*, Model 109, Campbell Scientific Inc., Logan, UT, USA), soil moisture (*Ms*, Model CS616, Campbell Scientific Inc., Logan, UT, USA), atmospheric radiation (CNR4, Zones Kipp & Zones B.V., Delft, The Netherlands), and soil heat flux (*Gn*, Model HFP01, Hukseflux, Delft, The Netherlands); where *Ts* and *Ms* are measured at 5-, 10-, 20-, and 40-cm soil depth, the AMS site only uses data of 20-cm layer due to probe damage, while the AS site does not use data of 40 cm. Atmospheric radiation observation includes upward and downward solar short-wave radiation and upward and downward long-wave radiation, which are used to calculate atmospheric net radiation. The data were processed by a CR1000X (Model Campbell Scientific Inc., Logan, UT, USA) and recorded every 10 min. Due to a failure of the solar power supply system, the AM site lacked effective *EC* observation data from 1 June to 30 June 2019. Since the changes of surface energy budget and *ET* during the growing season are mainly studied in this paper, the research results are basically not affected. *EC* system and automatic weather stations are powered by solar panels and batteries.

## 2.3. Data Processing

In this study, the half-hour turbulent flux was calculated, and the relevant flux was corrected according to the following steps: (1) The wild-point data were removed: before the flux was calculated, the original 10-Hz data were checked according to the method of Vickers and Mahrt [50], and the wild points that were far beyond the reasonable value or have obvious errors caused by instrument failure, weather influence, and random noise were eliminated. If the wild-point data in half an hour were greater than 10%, the flux in half an hour was regarded as vacant. (2) Coordinate rotation: a precondition for flux observation by *EC* is that the half-hour average value of vertical *WS* is zero, but this requirement cannot be met in actual observation due to terrain, instrument installation, and other factors. Therefore, the method of quadratic coordinate rotation was adopted to correct *WS* to meet the above conditions [51]. (3) Calculation of pulsation: the original data signal was split into

mean value and pulsation term using linear detrending method. (4) Frequency attenuation correction: according to the method introduced by Moncrieff [52], the systematic error of this part was corrected. (5) Density change correction: the open-circuit CO<sub>2</sub>/H<sub>2</sub>O analyzer measures the density of gas rather than the molar mixing ratio. The density change of air will affect the measurement of actual flux. The method introduced by Webb [53] was adopted to correct this part of error. (6) Turbulent flux measurement and correction: the analytical model proposed by Kormann and Meixner [54] was used to analyze the flux contribution area and eliminate the flux whose contribution to flux was less than 80% in the sample area. All the above steps are realized in EddyPro 5.2.0 software (LI-Cor, Lincoln, NE, USA).

Quality control was carried out for the calculated half-hour average flux. Firstly, the one-hour flux records before and after precipitation and snowfall were excluded. Then, Steady State Test and Integral Turbulence Characteristics Test were performed on half-hour original data according to Foken and Wichura's method [55]. Quality control was carried out on 10-min meteorological data obtained from AWS to ensure 144 data per day (every 10 min). In case of missing data, the value was set to null, and the time with repeated records was eliminated. Data obviously beyond the physical meaning or beyond the instrument range were deleted, and finally, we took the average value (except precipitation; in this case, we took the cumulative value) to get the data of half-an-hour scale.

In this study, the following methods were used to fill the vacancy flux data for estimation of the daily and monthly fluxes: for the vacancy less than or equal to 2 h, the linear difference was calculated according to the effective fluxes at both ends; a gap of more than 2 h was filled by mean diurnal variation with the observed mean value of 5 days in the same period before and after the neighboring period.

#### 2.4. Energy Balance and Evapotranspiration Calculation

In the determination of ecosystem energy flux by using EC observation, the surface-energy balance formula can be expressed as Equation (1):

$$LE + H = Rn - Gn \quad (1)$$

$$Rn = Rsd + Rld - Rsu - Rlu \quad (2)$$

where  $LE$  is the latent heat flux ( $W \cdot m^{-2}$ ),  $H$  is the sensible heat flux ( $W \cdot m^{-2}$ ),  $Rn$  is net radiation ( $W \cdot m^{-2}$ ), and  $Gn$  is soil heat flux ( $W \cdot m^{-2}$ ); and  $Rsd$ ,  $Rld$ ,  $Rsu$ , and  $Rlu$  are downward shortwave radiation, downward longwave radiation, upward shortwave radiation, and upward longwave radiation, respectively.

In this study,  $ET$  was calculated by Equations (3) and (4):

$$\lambda = (2500.78 - 2.3601 \times Ta) \times 1000 \quad (3)$$

$$ET = 3600 \times LE/\lambda \quad (4)$$

where  $\lambda$  is the latent heat of vaporization,  $Ta$  is air temperature ( $^{\circ}C$ ), and  $LE$  is latent heat ( $W \cdot m^{-2}$ ).

The percentage of  $ET_N$  is calculated by dividing  $ET_N$  by the total daily  $ET$ . Daytime (08:00–19:30) and nighttime (20:00–07:30) are divided according to Appel et al. [56]. The calculation of  $VPD$  is based on Equations (5) and (6) according to Wu et al. [57].

$$VPD = (1 - RH/100) \times SVP \quad (5)$$

$$SVP = 610.7 \times 10^{7.5Ta/(237.3+Ta)} \quad (6)$$

where  $RH$  is relative humidity, and  $SVP$  is the saturated vapor pressure for a given temperature ( $Ta$ ).

2.5. Statistic Analysis

We chose energy balance closure analysis to evaluate the reliability of the observed data by EC method. Linear regression method was used to the closure analysis of turbulent flux ( $LE + H$ ) and effective energy ( $Rn - Gn$ ) of the four ecosystems during the growing season from May to September in 2019. Additionally, data analysis was performed to assess the energy balance ratio (EBR) by Equation (7):

$$EBR = (LE + H)/(Rn - Gn) \tag{7}$$

Sensitivity analysis investigates the effect of change of one factor on another by its definition [58]. The sensitivity coefficient stands for the regression coefficient of each variable, which means the amount of change in ET caused by the variation of per unit in the variable. To explore the influencing factor of these ecosystems, partial least squares regression was used to calculate the sensitivity coefficient and contribution of  $Rn$ ,  $TD$ ,  $Ts$ ,  $-Pre$ ,  $VPD$ ,  $Ms$ ,  $WS$ , and  $NEE$  (daily scale data) to  $ET$  in daytime and nighttime, respectively. Then, the relative contribution is calculated by Equation (8):

$$RC_i = \frac{|R_i|}{\sum_{i=1}^n |R_i|} \times 100\% \tag{8}$$

where  $R_i$  is amount to the sensitivity coefficient,  $i$  represents the number of influence factors, and  $RC_i$  is the relative contribution of this impact factor.

The whole idea and methods of this study can be seen in Figure 2.

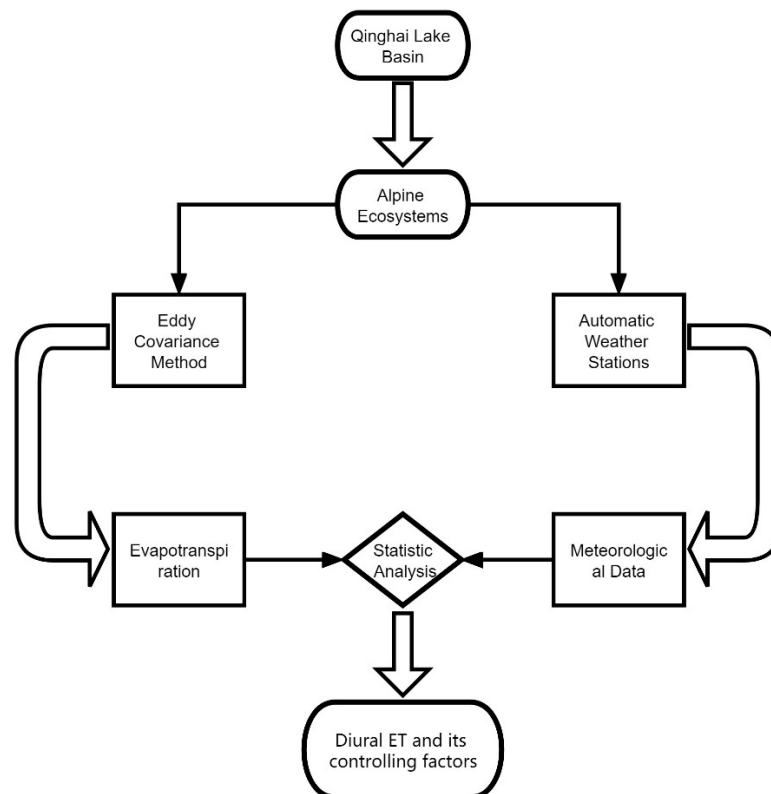


**Figure 2.** The flowchart of this study. Based on the half-hourly eddy covariance and micrometeorological data of four alpine ecosystems of the growing season (from May to September) in 2019 over Qinghai Lake Basin, their diurnal ET is quantified, and their influencing factors are identified during daytime and nighttime by statistical analysis method.

### 3. Results

#### 3.1. Energy Flux Closure

The average daily effective energy is  $163.30 \pm 67.60 \text{ W}\cdot\text{m}^{-2}$ ,  $129.61 \pm 49.98 \text{ W}\cdot\text{m}^{-2}$ ,  $121.37 \pm 51.25 \text{ W}\cdot\text{m}^{-2}$ , and  $158.20 \pm 62.35 \text{ W}\cdot\text{m}^{-2}$  at AD, AM, AMS, and AS sites, respectively, while the average daily of the turbulent flux is  $139.55 \pm 51.98 \text{ W}\cdot\text{m}^{-2}$ ,  $95.40 \pm 38.88 \text{ W}\cdot\text{m}^{-2}$ ,  $110.69 \pm 38.80 \text{ W}\cdot\text{m}^{-2}$ , and  $156.98 \pm 48.03 \text{ W}\cdot\text{m}^{-2}$  at AD, AM, AMS, and AS sites, respectively. Thus, the turbulent flux of all ecosystems was slightly lower than the effective energy, which indicated a 0.7~26.4% energy failure due to the instrumental measurement errors (Figure 3). Besides, linear regression coefficients of turbulent flux and effective energy shows *EBR* and *R*<sup>2</sup> ranged from 0.53~0.66 (with an average of 0.59) and 0.40~0.62 (Figure 3). That is, the observed flux datasets in those four alpine ecosystems are valid.

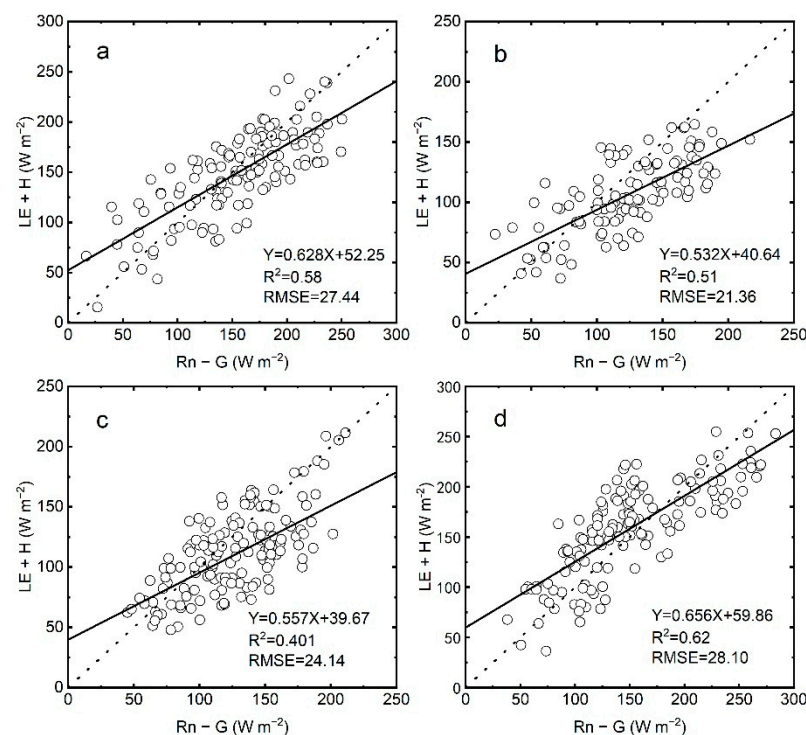


**Figure 3.** Energy balance closure of observation data at (a) alpine desert, (b) alpine meadow, (c) alpine meadow steppe, and (d) alpine steppe.

#### 3.2. Evapotranspiration in Different Ecosystems

The cumulative *ET* during the growing season of 2019 is 238.91 mm, 118.11 mm, 108.70 mm, and 240.18 mm at AD, AM, AMS, and AS sites, respectively, showing the highest *ET* at AS site and the lowest *ET* at AMS site (Figure 4a). The cumulative *ET<sub>N</sub>* is 28.97 mm, 13.09 mm, 16.39 mm, and 23.73 mm at AD, AM, AMS, and AS sites (Figure 4c), respectively, accounting for 9.88~15.08% (12.13%, 11.08%, 15.08%, and 9.88% for AD, AM, AMS, and AS sites, respectively) of total *ET* during the growing season (Figure 4d) and showing an order of cumulative *ET<sub>N</sub>* at AD > AS > AMS > AM; however, the highest rate of *ET<sub>N</sub>* was shown at AMS site and the lowest rate of *ET<sub>N</sub>* at AMS site. Besides, the rate of *ET<sub>N</sub>* to *ET* variety by month shows a divergent change with monthly *ET*. The monthly *ET* increased to its peak in July and August for the four alpine ecosystems (among them, the peak *ET* of AS site mainly in August and others in July), while the rate of *ET<sub>N</sub>* to *ET* reached the peak in June for AD site (with a rate of 18.18%), May for AM site (with a rate of 15.20%), June and September for AMS site (with a rate of 17.28% and 16.58%), and July for AS site (with a rate of 10.93%), respectively (Figure 4d).

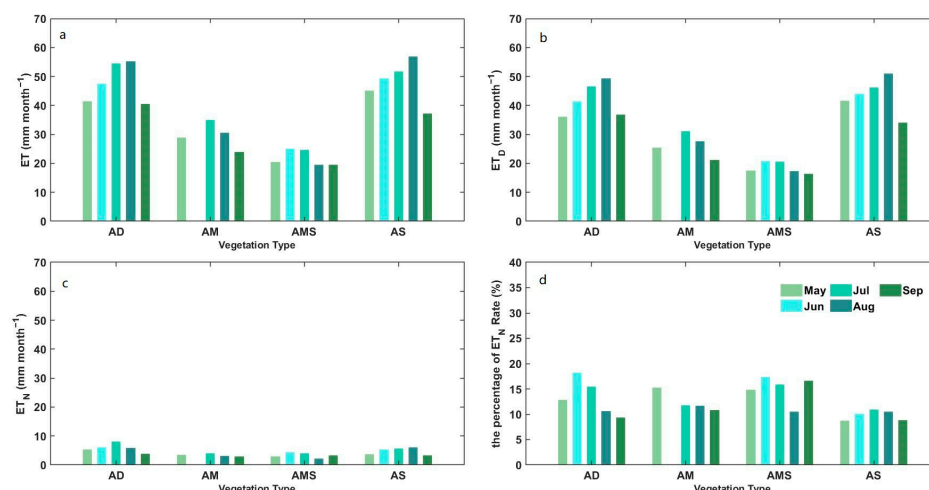


**Figure 4.** Monthly variation of (a) cumulative evapotranspiration ( $ET$ ), (b) cumulative evapotranspiration in daytime ( $ET_D$ ), (c) cumulative nocturnal evapotranspiration ( $ET_N$ ), and (d) the percentage of  $ET_N$  to  $ET$  of alpine ecosystems in the Qinghai Lake Basin during the growing season (from May to September) in 2019.

### 3.3. Influencing Factors for Evapotranspiration during Daytime and Nighttime

The controlling factors of  $ET$  during daytime and nighttime are different and vary among the four alpine ecosystems (Figures 5 and 6). In the daytime,  $VPD$  (with a sensitivity coefficient of 0.38,  $p < 0.01$ ),  $Ms$  (with a sensitivity coefficient of 0.23,  $p < 0.01$ ), and vegetation growth (with a sensitivity coefficient of  $-0.29$  between  $ET_D$  and  $NEE$ ,  $p < 0.05$ ) prominently promote  $ET_D$  at AD site (Figure 5a), and  $WS$  (with a sensitivity coefficient of 0.20 and 0.22 for AM and AMS sites, respectively,  $p < 0.01$ ) and  $Ms$  (with a sensitivity coefficient of 0.21 and 0.28 for AM and AMS sites, respectively,  $p < 0.05$ ) have a positive effect on  $ET_D$  both at AM and AMS sites (Figure 5a), while  $Ts$  is the main effect on the increase of  $ET_D$  at AS site (with a sensitivity coefficient of 0.31,  $p < 0.05$ ). Meanwhile,  $Rn$  and  $TD$  have a negative effect on  $ET_D$  at AM, AMS, and AS sites (Figure 5a). In the nighttime, the main influencing factors of  $ET_N$  in the four ecosystems include  $TD$ ,  $VPD$ , and  $WS$  (Figure 5b). Among them,  $TD$  has significant negative effect on  $ET_N$  at AD site (with a sensitivity coefficient of  $-0.31$ ,  $p < 0.01$ ) and AMS site (with a sensitivity coefficient of  $-0.44$ ,  $p < 0.05$ ) but promotes  $ET_N$  at AS site (with a sensitivity coefficient of 0.35,  $p < 0.01$ ) (Figure 5b);  $VPD$  (with a sensitivity coefficient of 0.47 and 0.27 for AD and AMS sites, respectively,  $p < 0.05$ ) and  $WS$  (with a sensitivity coefficient of 0.25 and 0.37 for AD and AMS sites, respectively,  $p < 0.05$ ) have a positive effect on  $ET_N$  both at AD and AMS sites in addition to the promoting of  $WS$  (with a sensitivity coefficient of 0.26,  $p < 0.05$ ) on  $ET_N$  at AS site (Figure 5b).

Besides, the relative contribution of the influencing factors of  $ET$  at high altitudes (AD and AM sites) and low altitude (AMS and AS sites) are calculated (Table 2). With a relative contribution over 15%,  $VPD$  (with a relative contribution of 20.30%),  $Rn$  (with a relative contribution of 19.15%), and  $Ms$  (with a relative contribution of 15.04%) are more important for controlling  $ET_D$  in daytime, and  $VPD$  (with a relative contribution of 24.85%),  $WS$  (with a relative contribution of 16.54%), and  $Ms$  (with a relative contribution of 15.53%) would be the main factor of  $ET_N$  in nighttime at high altitudes. While  $TD$  (with a relative contribution of 22.47%),  $Ts$  (with a relative contribution of 17.89%),  $WS$  (with a relative contribution of 15.82%), and  $Rn$  (with a relative contribution of 15.66%) have a sum of relative contribution of 71.84% on  $ET_D$  in daytime,  $TD$  (with a relative contribution of 26.14%) and  $WS$  (with a relative contribution of 20.81%) have a sum of relative contribution of 46.95% on  $ET_N$  in nighttime. That is,  $Rn$ ,  $TD$ ,  $VPD$ , and  $Ms$  have remarkable influence on  $ET_D$  in daytime, and  $Rn$  and  $VPD$  are more important at high altitudes, while  $TD$  is the main factor at low altitudes. In the nighttime,  $VPD$  and  $WS$  controlled  $ET_N$  at high altitudes, and  $TD$  and  $WS$  drove  $ET_N$  at low altitudes.



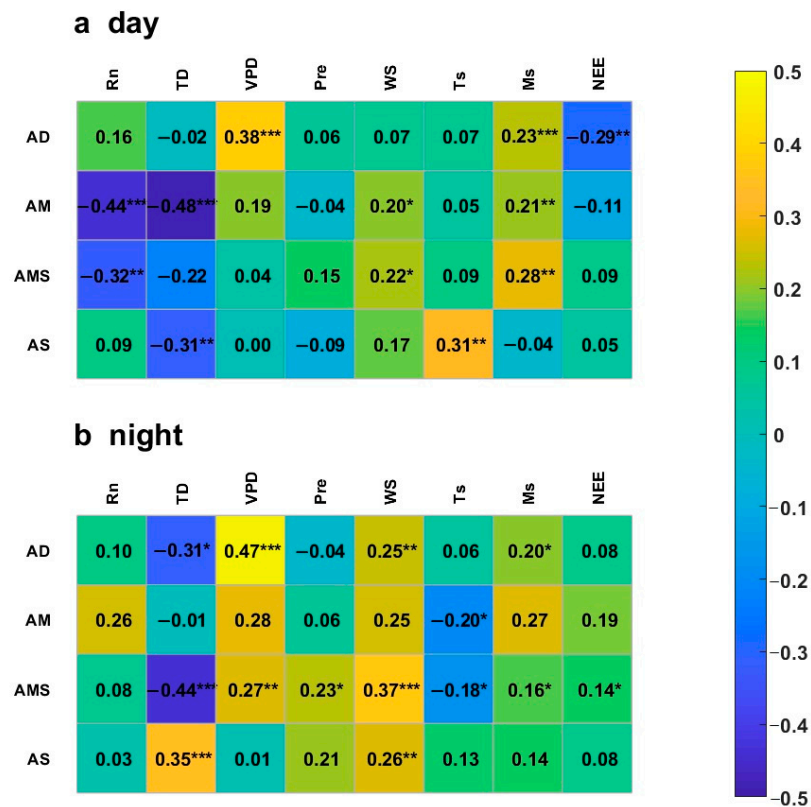


**Figure 5.** The sensitivity coefficient between daytime (a) and nighttime (b) climate factors and evapotranspiration at alpine desert (AD), alpine meadow (AM), alpine meadow steppe (AMS), and alpine steppe (AS) in the Qinghai Lake Basin. *Rn*, *TD*, *VPD*, *Pre*, *WS*, *Ts*, *Ms*, and *NEE* are the net radiation, temperature difference ( $T_a - LST$ ), vapor pressure difference, precipitation, wind speed, soil temperature, soil moisture, and net ecosystem exchange. \*, \*\*, and \*\*\* represent statistical significance at the  $p < 0.05$ ,  $p < 0.01$ , and  $p < 0.001$  levels, respectively.

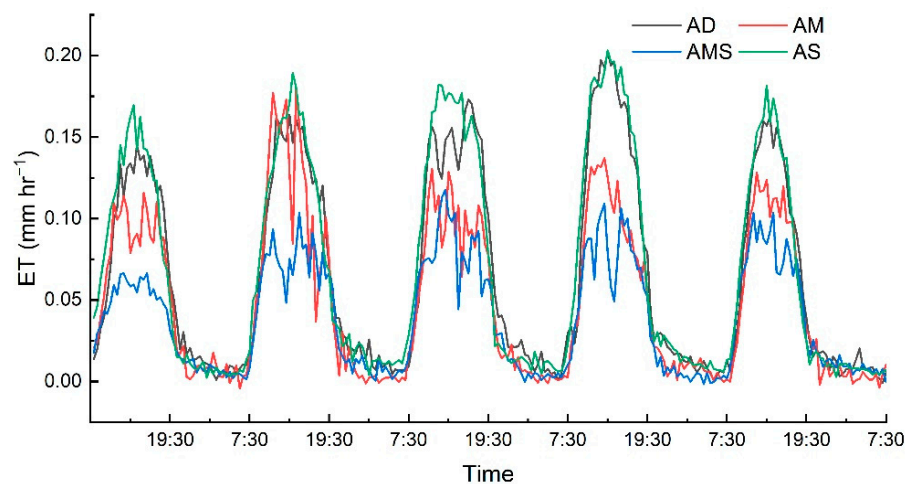


**Figure 6.** Diurnal variation of evapotranspiration of alpine desert (AD), alpine meadow (AM), alpine meadow steppe (AMS), and alpine steppe (AS) from May to September in 2019 in the Qinghai Lake Basin.

**Table 2.** The relative contribution (%) of each impact factor in daytime and nighttime at high and low altitudes.

Area	Time	<i>Rn</i>	<i>TD</i>	<i>VPD</i>	<i>Pre</i>	<i>Ts</i>	<i>Ms</i>	<i>WS</i>	<i>NEE</i>
high altitudes (>3800 m)	Daytime	19.15	14.56	20.30	3.68	4.21	15.04	8.68	14.38
	Nighttime	11.80	10.65	24.85	3.17	8.55	15.53	16.54	8.91
low altitudes (<3800 m)	Daytime	15.66	22.47	1.50	9.12	17.89	11.83	15.82	5.71
	Nighttime	3.19	26.14	7.71	14.86	10.23	9.99	20.81	7.08

*Rn*, *TD*, *VPD*, *Pre*, *WS*, *Ts*, *Ms*, and *NEE* are net radiation, temperature difference ( $T_a - LST$ ), vapor pressure difference, precipitation, wind speed, soil temperature, soil moisture, and net ecosystem exchange, respectively.

#### 4. Discussion

The evaluation of energy flux closure condition reflects the validity of *EC* observation to a certain extent [59,60]. Considering the instability of field observation, in general, the effect of eddy observation data is considered to be better than the *EBR* between turbulent flux, and effective flux is above 0.55 [61–64]. The slope of statistical regression of energy flux closure of all stations ranged from 0.53~0.66 in this study, which shows a bit lower slope. Different from other regions, the Qinghai-Tibet Plateau has high *WS* and wide temperature variation, which intensified the instability of *EC* observation [65,66]. By evaluating the energy closure of existing *EC* observations in China, Li et al. [67] suggested a lower acceptance coverage of the slope (0.55~0.99) in the Qinghai-Tibet Plateau.

$ET_N$  includes plant transpiration and soil evaporation as well as that in daytime [16,68]. However, high solar radiation leads to water loss at the daytime, while with the half-closed stomata of plants, *WS* is the main influencing factor of evaporation at night. Higher *WS* promotes the diffusion of water vapor molecules on the leaf surface and increases the *VPD* between the inside and outside of the leaf, thus promoting vegetation transpiration [7,8]. The incomplete closure of stomata on leaves would result in over 10% of daytime plant water loss at nighttime, and change of water potential caused by vertical soil temperature difference would lead to soil evaporation at night [12,15,69]. Thus,  $ET_N$  could occur in the nighttime when there is no solar radiation, and the soil temperature is low. Furthermore, some studies have observed the  $ET_N$ . For example, a study based on *EC* observation in United States showed that the average  $ET_N$  percentages were 8.0% in broadleaf forest, 9.1% in pine plantation, and 8.0% in old field environments [7]. Similarly, Guo et al. [25] pointed out that the average annual  $ET_N$  in shrubs in the arid region of northwest China was about 4% of the annual total *ET* during 2012–2014. Our observation results showed that evapotranspiration occupy 9.88~15.08% at night in the four stations, which is relatively higher than that above. That may be related to the fact that shrubs and trees are  $C_4$  plants whose metabolisms are inefficient in shady nighttime environments [12]. *ET* varies significantly with altitude in the basin [69–71]. Studies have shown that annual *ET* in alpine meadow reduced by 124.1 mm with an increase in elevation of 1000 m [49]. However, our result found growing season *ET* is higher at AS and AD than that at AM and AMS sites, which means no obvious trend of *ET* along with altitude. Different from the results on unified ecosystem, the discrepancy of microenvironment (such as species composition, hydrothermal conditions, and types and depth of frozen soil) would mean a different dominant factor of *ET* along with altitude [70,72]. Ma et al. [72] pointed out that the dominant factor of *ET* changed from water condition to temperature condition along with the altitude in the Qinghai Lake Basin, which means the main controlling factors of *ET* in the amount of a.l.s.<3560 m, 3650–3900 m, 3900–4350 m, and >4350 m are *Ms*,  $T_a$ , short-wave radiation, and  $T_a$ , respectively. However, apart from hydrothermal conditions, *ET* is also influenced by the boundary conditions between vegetation or soil surface and air, such as *WS*, *VPD*, and *TD*. Studies have shown that *WS* in arid and semi-arid areas of China shows a declining trend, and the declining *WS* will certainly weaken the local air flow, resulting in the decrease of *ET* [73,74]. In this study, the relative contribution of *TD* to  $ET_D$  is 22.47% in daytime, the sum relative contribution of *TD* and *WS* to  $ET_N$  is 46.95% in

nighttime at low altitudes, the sum relative contribution of  $VPD$  and  $Rn$  to  $ET_D$  is 39.45% in daytime, and the sum relative contribution of  $VPD$  and  $WS$  to  $ET_N$  is 40.38% at high altitudes, which suggests that  $ET$  is affected not only by hydrothermal condition but also by the dynamic factors, such as  $VPD$  and  $WS$ , especially in the alpine region. As for the effect of vegetation cover on  $ET$ ,  $Ta$  can regulate water and enzymatic activities in vegetation, which affects the evapotranspiration of vegetation [75]. The vegetation cover also prevents partial evaporation of soil water [76]. The dominant species in four alpine ecosystems are spaced regularly and low (the average height does not exceed 20 cm), but it still has an impact that cannot be ignored on  $ET$ . In this study,  $NEE$  has significant negative effect, which may be because the vegetation here needs more water on  $ET_D$  at AD site (with a sensitivity coefficient of  $-0.29$ ,  $p < 0.01$ ) but promotes  $ET_N$  because of more transpiration from the higher plants at AS site (with a sensitivity coefficient of  $0.14$ ,  $p < 0.05$ ).

Calculating  $ET$  by the method of energy balance may have a large relative error widely ranging from 10~20% [74,77], and the error could be higher under dry air conditions with lower gas flux [78,79]. Thus, we compared the  $ET$  from lysimeter and  $EC$  at the same experimental site in the Qinghai Lake Basin (Figure 7). During 11 February to 10 April in 2021, the total  $ET$ ,  $ET_N$ , and the percentage of  $ET_N$  recorded by lysimeter were 74.74 mm, 22.2 mm, and 21.38%, respectively, while the results of  $EC$  were 50.83 mm, 6.9 mm, and 13.91%, which are lower than that by lysimeter. With a relatively small space scale and higher time resolution, lysimeter is very sensitive to changes in weight, which would detect more elaborate  $ET$  processes and lead to a higher  $ET$  observation than that from  $EC$ , whose space scale is patch scale [80–82]. This suggests that the  $ET_N$  was underestimated, and its ratio and a higher value could be more reasonable in the Qinghai Lake Basin.

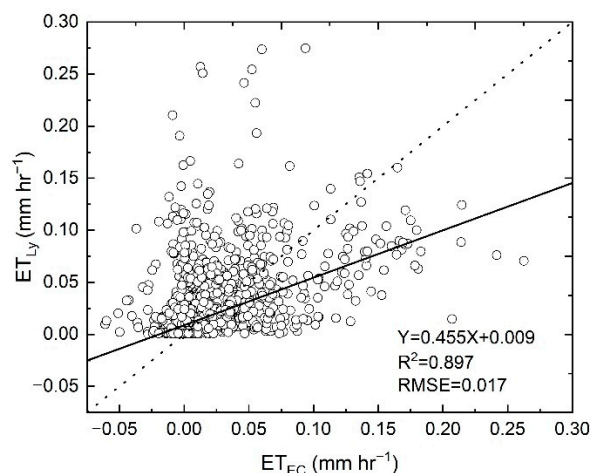


**Figure 7.** Comparison of evapotranspiration data measured by eddy covariance ( $ET_{EC}$ ) and lysimeter observation ( $ET_{Ly}$ ) at the same site in the Qinghai Lake Basin from 11 February to 10 April 2021.

## 5. Conclusions

In summary, based on the half-hour eddy and meteorological data of the growing season (from May to September) in 2019, the percentage of  $ET_N$  accounts for 9.88~15.08% of  $ET$ , and  $ET_N$  is relatively high with an order of AM (13.09 mm) < AMS (16.39 mm) < AS (23.73 mm) < AD (28.97 mm).  $VPD$ ,  $Ms$ , and  $NEE$  have a positive effect on  $ET_D$  at AD site;  $WS$  and  $Ms$  prominently promote  $ET_D$  both at AM and AMS sites; and  $Ts$  is the main influencing factor of the increase of  $ET_D$  at AS site. However,  $Rn$  and  $TD$  have a negative effect on  $ET_D$  at AM, AMS, and AS sites.  $TD$  has a significant negative effect on  $ET_N$  at AD and AMS sites but promotes  $ET_N$  at AS site;  $VPD$  and  $WS$  has a positive effect on  $ET_N$  both at AD and AMS sites in addition to the promotion of  $WS$  on  $ET_N$  at AS site. With a relative contribution of 22.47%,  $TD$  is more important for controlling  $ET_D$  in daytime, and the sum relative contribution of  $TD$  and  $WS$  to  $ET_N$  is 46.95% in nighttime at low altitudes, while the sum relative contribution of  $VPD$  and  $Rn$  to  $ET_D$  is 39.45% in daytime,

and the sum relative contribution of  $VPD$  and  $WS$  to  $ET_N$  is 40.38% at high altitudes. The findings of this study highlight the importance and significance of  $ET_N$ , which should be considered in evapotranspiration models, and is of great significance to the assessment of regional hydrological cycle and water resources. In future research,  $ET_N$  affected by water conditions or dynamic factors should not be ignored when estimating evapotranspiration of alpine ecosystems.

**Author Contributions:** Conceptualization, Q.L. and X.L.; methodology, F.S. and J.W.; validation, Q.L. and T.W.; investigation, F.Z.; data curation, F.S.; writing—original draft preparation, Q.L.; writing—review and editing, P.W. and Y.D.; supervision, X.L. All authors have read and agreed to the published version of the manuscript.

**Funding:** This research was funded by the National Natural Science Foundation of China (41971029), the Strategic Priority Research Program of the Chinese Academy of Sciences (Grant no. XDA20100102 and XDA20100101).

**Institutional Review Board Statement:** Not applicable.

**Informed Consent Statement:** Not applicable.

**Data Availability Statement:** The data presented in this study are not publicly available, but readers in need can contact with the corresponding author (xyli@bnu.edu.cn).

**Conflicts of Interest:** The authors declare no conflict of interest.

## References

- Gu, L.; Hu, Z.; Yao, J.; Sun, G. Actual and Reference Evapotranspiration in a Cornfield in the Zhangye Oasis, Northwestern China. *Water* **2017**, *9*, 499. [[CrossRef](#)]
- Javadian, M.; Behrangi, A.; Smith, W.K.; Fisher, J.B. Global Trends in Evapotranspiration Dominated by Increases across Large Cropland Regions. *Remote Sens.* **2020**, *12*, 1221. [[CrossRef](#)]
- Mackay, D.S.; Ahl, D.E.; Ewers, B.E.; Gower, S.T.; Burrows, S.N.; Samanta, S.; Davis, K.J. Effects of aggregated classifications of forest composition on estimates of evapotranspiration in a northern Wisconsin forest. *Glob. Chang. Biol.* **2002**, *8*, 1253–1265. [[CrossRef](#)]
- Soppe, R.; Ayars, J. Characterizing ground water use by safflower using weighing lysimeters. *Agric. Water Manag.* **2003**, *60*, 59–71. [[CrossRef](#)]
- Iritz, Z.; Lindroth, A. Night-time evaporation from a short-rotation willow stand. *J. Hydrol.* **1994**, *157*, 235–245. [[CrossRef](#)]
- Monteith, J. Evaporation at night. *Neth. J. Agric. Sci.* **1956**, *4*, 34–38. [[CrossRef](#)]
- Novick, K.; Oren, R.; Stoy, P.; Siqueira, M.; Katul, G. Nocturnal evapotranspiration in eddy-covariance records from three co-located ecosystems in the Southeastern U.S.: Implications for annual fluxes. *Agric. For. Meteorol.* **2009**, *149*, 1491–1504. [[CrossRef](#)]
- Buckley, T.N.; Turnbull, T.L.; Pfautsch, S.; Adams, M.A. Nocturnal water loss in mature subalpine *Eucalyptus delegatensis* tall open forests and adjacent *E. pauciflora* woodlands. *Ecol. Evol.* **2011**, *1*, 435–450. [[CrossRef](#)]
- Barbeta, A.; Ogaya, R.; Peñuelas, J. Comparative study of diurnal and nocturnal sap flow of *Quercus ilex* and *Phillyrea latifolia* in a Mediterranean holm oak forest in Prades (Catalonia, NE Spain). *Trees* **2012**, *26*, 1651–1659. [[CrossRef](#)]
- Montoro, A.; Mañas, F.; López-Urrea, R. Transpiration and evaporation of grapevine, two components related to irrigation strategy. *Agric. Water Manag.* **2016**, *177*, 193–200. [[CrossRef](#)]
- Ramírez, D.A.; Yactayo, W.; Rolando, J.L.; Quiroz, R. Correction to: Preliminary Evidence of Nocturnal Transpiration and Stomatal Conductance in Potato and their Interaction with Drought and Yield. *Am. Potato J.* **2017**, *95*, 139–143. [[CrossRef](#)]
- Caird, M.A.; Richards, J.H.; Donovan, L. Nighttime Stomatal Conductance and Transpiration in  $C_3$  and  $C_4$  Plants. *Plant Physiol.* **2007**, *143*, 4–10. [[CrossRef](#)] [[PubMed](#)]
- Bucci, S.J.; Scholz, F.G.; Goldstein, G.; Meinzer, F.; Hinojosa, J.A.; Hoffmann, W.A.; Franco, A. Processes preventing nocturnal equilibration between leaf and soil water potential in tropical savanna woody species. *Tree Physiol.* **2004**, *24*, 1119–1127. [[CrossRef](#)] [[PubMed](#)]
- Ogle, K.; Lucas, R.W.; Bentley, L.P.; Cable, J.M.; Barron-Gafford, G.A.; Griffith, A.; Ignace, D.; Jenerette, G.D.; Tyler, A.; Huxman, T.E.; et al. Differential daytime and night-time stomatal behavior in plants from North American deserts. *New Phytol.* **2012**, *194*, 464–476. [[CrossRef](#)]
- Milly, P.C.D. Moisture and heat transport in hysteretic, inhomogeneous porous media: A matric head-based formulation and a numerical model. *Water Resour. Res.* **1982**, *18*, 489–498. [[CrossRef](#)]
- Balugani, E.; Lubczynski, M.; van der Tol, C.; Metselaar, K. Testing three approaches to estimate soil evaporation through a dry soil layer in a semi-arid area. *J. Hydrol.* **2018**, *567*, 405–419. [[CrossRef](#)]

17. Meng, Y.; He, Z.; Liu, B.; Chen, L.; Lin, P.; Luo, W. Soil Salinity and Moisture Control the Processes of Soil Nitrification and Denitrification in a Riparian Wetlands in an Extremely Arid Regions in Northwestern China. *Water* **2020**, *12*, 2815. [[CrossRef](#)]
18. Brown, C.; Devitt, D.; Morris, R. Water Use and Physiological Response of Tall Fescue Turf to Water Deficit Irrigation in an Arid Environment. *HortScience* **2004**, *39*, 388–393. [[CrossRef](#)]
19. Zhang, W.; Chen, S.; Chen, J.; Wei, L.; Han, X.; Lin, G. Biophysical regulations of carbon fluxes of a steppe and a cultivated cropland in semiarid Inner Mongolia. *Agric. For. Meteorol.* **2007**, *146*, 216–229. [[CrossRef](#)]
20. Li, X.W.; Zhou, J.L.; Jin, M.G.; Liu, Y.F.; Li, Q. Experiments on Evaporation of High-TDS Phreatic Water in an Arid Area. *Adv. Mater. Res.* **2012**, *446–449*, 2815–2823. [[CrossRef](#)]
21. Rebetz, M.; Reinhard, M. Monthly air temperature trends in Switzerland 1901–2000 and 1975–2004. *Theor. Appl. Climatol.* **2007**, *91*, 27–34. [[CrossRef](#)]
22. Williams, M.W.; Losleben, M.V.; Hamann, H.B. Alpine Areas in the Colorado Front Range as Monitors of Climate Change and Ecosystem Response. *Geogr. Rev.* **2002**, *92*, 180–191. [[CrossRef](#)]
23. Christopher, T.A.; Goodburn, J.M. The Effects of Spatial Patterns on the Accuracy of Forest Vegetation Simulator (FVS) Estimates of Forest Canopy Cover. *West. J. Appl. For.* **2008**, *23*, 5–11. [[CrossRef](#)]
24. Tie, Q.; Hu, H.; Tian, F.; Holbrook, N.M. Comparing different methods for determining forest evapotranspiration and its components at multiple temporal scales. *Sci. Total Environ.* **2018**, *633*, 12–29. [[CrossRef](#)] [[PubMed](#)]
25. Guo, Y.; Song, C.; Zhang, J.; Wang, L.; Sun, L. Influence of wetland reclamation on land-surface energy exchange and evapotranspiration in the Sanjiang plain, Northeast China. *Agric. For. Meteorol.* **2021**, *296*, 108214. [[CrossRef](#)]
26. Zhang, Z.; Li, X.; Liu, L.; Wang, Y.; Li, Y. Influence of mulched drip irrigation on landscape scale evapotranspiration from farmland in an arid area. *Agric. Water Manag.* **2020**, *230*, 105953. [[CrossRef](#)]
27. Mostafa, H.; El-Nady, R.; Awad, M.; El-Ansary, M. Drip irrigation management for wheat under clay soil in arid conditions. *Ecol. Eng.* **2018**, *121*, 35–43. [[CrossRef](#)]
28. Wang, F.; Liang, W.; Fu, B.; Jin, Z.; Yan, J.; Zhang, W.; Fu, S.; Yan, N. Changes of cropland evapotranspiration and its driving factors on the loess plateau of China. *Sci. Total Environ.* **2020**, *728*, 138582. [[CrossRef](#)]
29. Yang, K.; Wu, H.; Qin, J.; Lin, C.; Tang, W.; Chen, Y. Recent climate changes over the Tibetan Plateau and their impacts on energy and water cycle: A review. *Glob. Planet. Chang.* **2014**, *112*, 79–91. [[CrossRef](#)]
30. Zhong, L.; Ma, Y.; Salama, M.S.; Su, Z. Assessment of vegetation dynamics and their response to variations in precipitation and temperature in the Tibetan Plateau. *Clim. Chang.* **2010**, *103*, 519–535. [[CrossRef](#)]
31. Zhang, R.; Zuo, Z. Impact of Spring Soil Moisture on Surface Energy Balance and Summer Monsoon Circulation over East Asia and Precipitation in East China. *J. Clim.* **2011**, *24*, 3309–3322. [[CrossRef](#)]
32. Yin, Y.; Wu, S.; Zhao, D.; Zheng, D.; Pan, T. Modeled effects of climate change on actual evapotranspiration in different eco-geographical regions in the Tibetan Plateau. *J. Geogr. Sci.* **2013**, *23*, 195–207. [[CrossRef](#)]
33. Guerschman, J.P.; Van Dijk, A.I.J.M.; Mattersdorf, G.; Beringer, J.; Hutley, L.B.; Leuning, R.; Pipunic, R.C.; Sherman, B.S. Scaling of potential evapotranspiration with MODIS data reproduces flux observations and catchment water balance observations across Australia. *J. Hydrol.* **2009**, *369*, 107–119. [[CrossRef](#)]
34. Koppa, A.; Alam, S.; Miralles, D.G.; Gebremichael, M. Budyko-Based Long-Term Water and Energy Balance Closure in Global Watersheds From Earth Observations. *Water Resour. Res.* **2021**, *57*, e2020WR028658. [[CrossRef](#)] [[PubMed](#)]
35. McCabe, M.F.; Miralles, D.G.; Holmes, T.R.; Fisher, J.B. Advances in the Remote Sensing of Terrestrial Evaporation. *Remote Sens.* **2019**, *11*, 1138. [[CrossRef](#)]
36. Srivastava, A.; Sahoo, B.; Raghuvanshi, N.S.; Singh, R. Evaluation of Variable-Infiltration Capacity Model and MODIS-Terra Satellite-Derived Grid-Scale Evapotranspiration Estimates in a River Basin with Tropical Monsoon-Type Climatology. *J. Irrig. Drain. Eng.* **2017**, *143*, 04017028. [[CrossRef](#)]
37. Douglas, E.M.; Jacobs, J.M.; Sumner, D.M.; Ray, R.L. A comparison of models for estimating potential evapotranspiration for Florida land cover types. *J. Hydrol.* **2009**, *373*, 366–376. [[CrossRef](#)]
38. Federer, C.A.; Vörösmarty, C.; Fekete, B. Intercomparison of Methods for Calculating Potential Evaporation in Regional and Global Water Balance Models. *Water Resour. Res.* **1996**, *32*, 2315–2321. [[CrossRef](#)]
39. Wilson, K.B.; Hanson, P.J.; Mulholland, P.J.; Baldocchi, D.D.; Wullschleger, S.D. A comparison of methods for determining forest evapotranspiration and its components: Sap-flow, soil water budget, eddy covariance and catchment water balance. *Agric. For. Meteorol.* **2001**, *106*, 153–168. [[CrossRef](#)]
40. Hicks, B.B.; Baldocchi, D.D. Measurement of Fluxes over Land: Capabilities, Origins, and Remaining Challenges. *Bound. Layer Meteorol.* **2020**, *177*, 365–394. [[CrossRef](#)]
41. Cheng, L.; Xu, Z.; Wang, D.; Cai, X. Assessing interannual variability of evapotranspiration at the catchment scale using satellite-based evapotranspiration data sets. *Water Resour. Res.* **2011**, *47*, 09509. [[CrossRef](#)]
42. Chai, R.; Sun, S.; Chen, H.; Zhou, S. Changes in reference evapotranspiration over China during 1960–2012: Attributions and relationships with atmospheric circulation. *Hydrol. Process.* **2018**, *32*, 3032–3048. [[CrossRef](#)]
43. Sun, X.; Zou, C.B.; Wilcox, B.; Stebler, E. Effect of Vegetation on the Energy Balance and Evapotranspiration in Tallgrass Prairie: A Paired Study Using the Eddy-Covariance Method. *Bound. Layer Meteorol.* **2018**, *170*, 127–160. [[CrossRef](#)]
44. Li, X.; Yang, X.; Ma, Y.; Hu, G.; Hu, X.; Wu, X.; Wang, P.; Huang, Y.; Cui, B.; Wei, J. Qinghai Lake Basin Critical Zone Observatory on the Qinghai-Tibet Plateau. *Vadose Zone J.* **2018**, *17*, 1–11. [[CrossRef](#)]

45. Huang, C.; Lai, Z.; Liu, X.; Madsen, D. Lake-level history of Qinghai Lake on the NE Tibetan Plateau and its implications for Asian monsoon pattern—A review. *Quat. Sci. Rev.* **2021**, *273*, 107258. [[CrossRef](#)]
46. Wang, Z.; Cao, S.; Cao, G.; Lan, Y. Effects of vegetation phenology on vegetation productivity in the Qinghai Lake Basin of the Northeastern Qinghai-Tibet Plateau. *Arab. J. Geosci.* **2021**, *14*, 1–15. [[CrossRef](#)]
47. Duan, H.; Xue, X.; Wang, T.; Kang, W.; Liao, J.; Liu, S. Spatial and Temporal Differences in Alpine Meadow, Alpine Steppe and All Vegetation of the Qinghai-Tibetan Plateau and Their Responses to Climate Change. *Remote Sens.* **2021**, *13*, 669. [[CrossRef](#)]
48. Zhang, S.-Y.; Li, X.-Y. Soil moisture and temperature dynamics in typical alpine ecosystems: A continuous multi-depth measurements-based analysis from the Qinghai-Tibet Plateau, China. *Hydrol. Res.* **2018**, *49*, 194–209. [[CrossRef](#)]
49. Cao, S.; Cao, G.; Han, G.; Wu, F.; Lan, Y. Comparison of evapotranspiration between two alpine type wetland ecosystems in Qinghai lake basin of Qinghai-Tibet Plateau. *Ecohydrol. Hydrobiol.* **2020**, *20*, 215–229. [[CrossRef](#)]
50. Vickers, D.; Mahrt, L. Quality control and flux sampling problems for tower and aircraft data. *J. Atmos. Ocean. Tech.* **1997**, *14*, 512–526. [[CrossRef](#)]
51. Mason, P. Atmospheric boundary layer flows: Their structure and measurement. *Bound. Layer Meteorol.* **1995**, *72*, 213–214. [[CrossRef](#)]
52. Moncrieff, J.; Massheder, J.; de Bruin, H.; Elbers, J.; Friborg, T.; Heusinkveld, B.; Kabat, P.; Scott, S.; Soegaard, H.; Verhoef, A. A system to measure surface fluxes of momentum, sensible heat, water vapour and carbon dioxide. *J. Hydrol.* **1997**, *188–189*, 589–611. [[CrossRef](#)]
53. Webb, E.K.; Pearman, G.I.; Leuning, R. Correction of flux measurements for density effects due to heat and water vapour transfer. *Q. J. R. Meteorol. Soc.* **1980**, *106*, 85–100. [[CrossRef](#)]
54. Kormann, R.; Meixner, F.X. An Analytical Footprint Model For Non-Neutral Stratification. *Bound. Layer Meteorol.* **2001**, *99*, 207–224. [[CrossRef](#)]
55. Foken, T.; Wichura, B. Tools for quality assessment of surface-based flux measurements. *Agric. For. Meteorol.* **1996**, *78*, 83–105. [[CrossRef](#)]
56. Appel, K.W.; Chemel, C.; Roselle, S.; Francis, X.V.; Hu, R.-M.; Sokhi, R.S.; Rao, S.; Galmarini, S. Examination of the Community Multiscale Air Quality (CMAQ) model performance over the North American and European domains. *Atmos. Environ.* **2012**, *53*, 142–155. [[CrossRef](#)]
57. Wu, X.; Liu, H.; Li, X.; Ciais, P.; Babst, F.; Guo, W.; Zhang, C.; Magliulo, V.; Pavelka, M.; Liu, S.; et al. Differentiating drought legacy effects on vegetation growth over the temperate Northern Hemisphere. *Glob. Chang. Biol.* **2018**, *24*, 504–516. [[CrossRef](#)]
58. McCuen, R.H. A sensitivity and error analysis of procedures used for estimating evaporation. *JAWRA J. Am. Water Resour. Assoc.* **1974**, *10*, 486–497. [[CrossRef](#)]
59. Eder, F.; De Roo, F.; Kohnert, K.; Desjardins, R.L.; Schmid, H.P.; Mauder, M. Evaluation of Two Energy Balance Closure Parametrizations. *Bound. Layer Meteorol.* **2014**, *151*, 195–219. [[CrossRef](#)]
60. Sun, X.-M.; Zhu, Z.-L.; Wen, X.-F.; Yuan, G.-F.; Yu, G.-R. The impact of averaging period on eddy fluxes observed at China FLUX sites. *Agric. For. Meteorol.* **2006**, *137*, 188–193. [[CrossRef](#)]
61. Yu, G.-R.; Wen, X.-F.; Sun, X.-M.; Tanner, B.D.; Lee, X.; Chen, J.-Y. Overview of China FLUX and evaluation of its eddy covariance measurement. *Agric. For. Meteorol.* **2006**, *137*, 125–137. [[CrossRef](#)]
62. Shi, T.; Guan, D.; Wang, A.; Wu, J.; Jin, C.; Han, S. Comparison of three models to estimate evapotranspiration for a temperate mixed forest. *Hydrol. Process.* **2008**, *22*, 3431–3443. [[CrossRef](#)]
63. Wu, J.; Jing, Y.; Guan, D.; Yang, H.; Niu, L.; Wang, A.; Yuan, F.; Jin, C. Controls of evapotranspiration during the short dry season in a temperate mixed forest in Northeast China. *Ecohydrology* **2012**, *6*, 775–782. [[CrossRef](#)]
64. Yan, C.; Zhao, W.; Wang, Y.; Yang, Q.; Zhang, Q.; Qiu, G.Y. Effects of forest evapotranspiration on soil water budget and energy flux partitioning in a subalpine valley of China. *Agric. For. Meteorol.* **2017**, *246*, 207–217. [[CrossRef](#)]
65. Xin, Y.-F.; Chen, F.; Zhao, P.; Barlage, M.; Blanken, P.; Chen, Y.-L.; Chen, B.; Wang, Y.-J. Surface energy balance closure at ten sites over the Tibetan plateau. *Agric. For. Meteorol.* **2018**, *259*, 317–328. [[CrossRef](#)]
66. Wang, K.C.; Dickinson, R.E. A review of global terrestrial evapotranspiration: Observation, modeling, climatology, and climatic variability. *Rev. Geophys.* **2012**, *50*, RG2005. [[CrossRef](#)]
67. Li, M.; Babel, W.; Chen, X.; Zhang, L.; Sun, F.; Wang, B.; Ma, Y.; Hu, Z.; Foken, T. A 3-year dataset of sensible and latent heat fluxes from the Tibetan Plateau, derived using eddy covariance measurements. *Theor. Appl. Climatol.* **2015**, *122*, 457–469. [[CrossRef](#)]
68. Montoro, A.; Torija, I.; Mañas, F.; López-Urrea, R. Lysimeter measurements of nocturnal and diurnal grapevine transpiration: Effect of soil water content, and phenology. *Agric. Water Manag.* **2020**, *229*, 105882. [[CrossRef](#)]
69. Li, H.-J.; Yan, J.-X.; Yue, X.-F.; Wang, M.-B. Significance of soil temperature and moisture for soil respiration in a Chinese mountain area. *Agric. For. Meteorol.* **2008**, *148*, 490–503. [[CrossRef](#)]
70. Goulden, M.L.; Bales, R.C. Mountain runoff vulnerability to increased evapotranspiration with vegetation expansion. *Proc. Natl. Acad. Sci. USA* **2014**, *111*, 14071–14075. [[CrossRef](#)]
71. Cao, S.; Cao, G.; Chen, K.; Han, G.; Liu, Y.; Yang, Y.; Li, X. Characteristics of CO<sub>2</sub>, water vapor, and energy exchanges at a headwater wetland ecosystem of the Qinghai Lake. *Can. J. Soil Sci.* **2019**, *99*, 227–243. [[CrossRef](#)]
72. Ma, Y.-J.; Li, X.-Y.; Liu, L.; Yang, X.-F.; Wu, X.-C.; Wang, P.; Lin, H.; Zhang, G.-H.; Miao, C.-Y. Evapotranspiration and its dominant controls along an elevation gradient in the Qinghai Lake watershed, northeast Qinghai-Tibet Plateau. *J. Hydrol.* **2019**, *575*, 257–268. [[CrossRef](#)]

73. Shi, Z.; Xu, L.; Yang, X.; Guo, H.; Dong, L.; Song, A.; Zhang, X.; Shan, N. Trends in reference evapotranspiration and its attribution over the past 50 years in the Loess Plateau, China: Implications for ecological projects and agricultural production. *Stoch. Environ. Res. Risk A* **2017**, *31*, 257–273. [[CrossRef](#)]
74. Irmak, S. Dynamics of Nocturnal, Daytime, and Sum-of-Hourly Evapotranspiration and Other Surface Energy Fluxes over Nonstressed Maize Canopy. *J. Irrig. Drain. Eng.* **2011**, *137*, 475–490. [[CrossRef](#)]
75. Zhang, P.; Cai, Y.; Yang, W.; Yi, Y.; Yang, Z.; Fu, Q. Multiple spatiotemporal patterns of vegetation coverage and its relationship with climatic factors in a large dam-reservoir-river system. *Ecol. Eng.* **2019**, *138*, 188–199. [[CrossRef](#)]
76. Wang, Y.; Liu, Y.; Jin, J. Contrast Effects of Vegetation Cover Change on Evapotranspiration during a Revegetation Period in the Poyang Lake Basin, China. *Forests* **2018**, *9*, 217. [[CrossRef](#)]
77. Stannard, D.I.; Blanford, J.H.; Kustas, W.P.; Nichols, W.D.; Amer, S.A.; Schmugge, T.J.; Weltz, M.A. Interpretation of surface flux measurements in heterogeneous terrain during the Monsoon '90 experiment. *Water Resour. Res.* **1994**, *30*, 1227–1239. [[CrossRef](#)]
78. Mahrt, L. Flux Sampling Errors for Aircraft and Towers. *J. Atmos. Ocean. Technol.* **1998**, *15*, 416–429. [[CrossRef](#)]
79. Moore, K.E.; Fitzjarrald, D.R.; Sakai, R.K.; Goulden, M.L.; Munger, J.W.; Wofsy, S.C. Seasonal Variation in Radiative and Turbulent Exchange at a Deciduous Forest in Central Massachusetts. *J. Appl. Meteorol. Clim.* **1996**, *35*, 122–134. [[CrossRef](#)]
80. De Dios, V.R.; Roy, J.; Ferrio, J.P.; Alday, J.G.; Landais, D.; Milcu, A.; Gessler, A. Processes driving nocturnal transpiration and implications for estimating land evapotranspiration. *Sci. Rep. UK* **2015**, *5*, 1–8. [[CrossRef](#)]
81. Han, Y.; Zhang, L.; Wang, C.; Yuan, J.; Wei, H. Dynamic characteristics and influencing factors of actual evapotranspiration in cold wetland. *South North. Water Transf. Water Sci. Technol.* **2018**, *16*, 28–34. [[CrossRef](#)]
82. Oishi, A.C.; Oren, R.; Stoy, P.C. Estimating components of forest evapotranspiration: A footprint approach for scaling sap flux measurements. *Agric. For. Meteorol.* **2008**, *148*, 1719–1732. [[CrossRef](#)]